Supporting Information

Synthesis, Structures, and Some Properties of Diiron Oxadiselenolate (ODSe) and Thiodiselenolate (TDSe) Complexes as Models for the Active Site of [FeFe]-Hydrogenases

Li-Cheng Song,* Bin Gai, Zhan-Heng Feng, Zong-Qiang Du, Zhao-Jun Xie, Xiao-Jing Sun, and Hai-Bin Song
Department of Chemistry, State Key Laboratory of Elemento-Organic Chemistry, Nankai University, Tianjin 300071, China
E-mail: lcsong@nankai.edu.cn

The Supporting Information contains:

1. **Table S1. Selected Bond Lengths (Å) and Angles (deg) for B**
2. **Table S2. Crystal Data and Structure Refinements Details for B**
3. **Table S3. Crystal Data and Structure Refinements Details for A, 1 and 2**
4. **Table S4. Crystal Data and Structure Refinements Details for 3, 4, 6 and 7**
5. **Table S5. Crystal Data and Structure Refinements Details for 8–10**
6. **Figure S1. ORTEP view of B with 30% probability level ellipsoids.**
7. **Figure S2. Cyclic voltammogram of a mixture of A (1.0 mM) and ferrocene (1.0 mM) in 0.1 M *n*-Bu_4NPF_6/MeCN at a scan rate of 0.1 $V\cdot s^{-1}$.**
8. **Figure S3. Cyclic voltammogram of a mixture of B (1.0 mM) and ferrocene (1.0 mM) in 0.1 M *n*-Bu_4NPF_6/MeCN at a scan rate of 0.1 $V\cdot s^{-1}$.**
9. **Figure S4. CPC for the two-electron reduction of $[CpFe(CO)_2]_2$ and the first reductions of A and B.**
10. **Figure S5. CPC for the two-electron reduction of $[CpFe(CO)_2]_2$ and the oxidations of A and B.**
11. **Figure S6. Cyclic voltammograms of (μ-ODT)$Fe_2(CO)_6$ (1.0 mM) with HOAc (0–10 mM) in 0.1 M *n*-Bu_4NPF_6/MeCN at a scan rate of 0.1 $V\cdot s^{-1}$**
12. **Figure S7. Cyclic voltammograms of (μ-TDT)$Fe_2(CO)_6$ (1.0 mM) with HOAc (0–10 mM) in 0.1 M *n*-Bu_4NPF_6/MeCN at a scan rate of 0.1 $V\cdot s^{-1}$**

Table S1. Selected Bond Lengths (Å) and Angles (deg) for B

Se(1)–C(8)	1.980(4)	Fe(1)–Se(2)	2.3721(6)
Se(1)–Fe(1)	2.3659(8)	Se(2)–Fe(1A)	2.3721(6)
Se(1)–Fe(1A)	2.3659(8)	Fe(1)–Fe(1A)	2.5600(9)
Se(2)–C(7)	1.977(4)	C(7)–S(1)	1.721(3)
Fe(1)–Se(1)–Fe(1A)	65.51(3)	Se(2)–Fe(1)–Fe(1A)	57.342(12)
Fe(1)–Se(2)–Fe(1A)	65.32(2)	C(7)–S(1)–C(8)	101.92(16)
Se(1)–Fe(1)–Se(2)	87.95(2)	S(1)–C(7)–Se(2)	120.02(19)
Se(1)–Fe(1)–Fe(1A)	57.247(15)	C(1)–Fe(1)–Se(1)	103.43(9)

Table S2. Crystal Data and Structure Refinements Details for B

mol formula	$C_8H_4Fe_2O_6SSe_2$
mol wt	497.79
cryst syst	monoclinic
space group	P21/m
a /Å	6.9473(14)
b /Å	13.261(3)
c /Å	8.0038(16)
α /deg	90
β /deg	108.60(3)
γ /deg	90
V/Å^3	698.9(3)
Z	2
Dc/g·cm^{-3}	2.366
abs coeff/mm^{-1}	7.447
F(000)	472
index ranges	$-9 \le h \le 9$
	$-17 \le k \le 10$,
	$-10 \le l \le 10$
no. of reflns	5061
no. of indep reflns	1726
$2\theta_{max}$ /deg	55.80
R	0.0234
Rw	0.0609
goodness of fit	1.054
largest diff peak and hole/e Å^{-3}	0.539/−1.058

Table S3. Crystal Data and Structure Refinements Details for A, 1 and 2

	A	1	2
mol formula	$C_8H_4Fe_2O_7Se_2$	$C_{25}H_{19}Fe_2O_6PSe_2$	$C_{20}H_{17}Fe_2O_7PSe_2$
mol wt	481.73	715.99	669.3
cryst syst	monoclinic	monoclinic	triclinic
space group	P2(1)	P2(1)/n	P−1
a /Å	6.8642(14)	11.239(2)	8.2079(16)
b /Å	13.424(3)	21.512(4)	10.782(2)
c /Å	7.7612(16)	12.057(2)	13.742(3)
α /deg	90	90	99.86(3)
β /deg	110.67(3)	116.91(3)	95.20(3)
γ /deg	90	90	100.43(3)
V/Å^3	669.1(2)	2599.4(9)	1169.0(4)
Z	2	4	2
D_c/g·cm^{-3}	2.391	1.830	1.903
abs coeff/mm^{-1}	7.629	4.017	4.461
F(000)	456	1408	656
index ranges	$-8 \le h \le 8$	$-13 \le h \le 13$	$-9 \le h \le 8$
	$-17 \le k \le 17$	$-25 \le k \le 25$	$-12 \le k \le 12$
	$-10 \le l \le 6$	$-13 \le l \le 14$	$-16 \le l \le 16$
no. of reflns	5523	19015	8701
no. of indep reflns	1643	4594	4105
$2\theta_{max}$ /deg	55.68	50.04	50.04
R	0.0445	0.0429	0.0341
R_w	0.0876	0.0981	0.0683
goodness of fit	0.712	1.041	1.024
largest diff peak, hole/e Å^{-3}	1.472/−1.942	0.863/−0.639	0.467/−0.582

Table S4. Crystal Data and Structure Refinements Details for 3, 4, 6 and 7

	3	4	6	7
mol formula	$C_{28}H_{28}Fe_2N_2O_6Se_2$	$C_{20}H_{20}Fe_2N_2O_6Se_2$	$C_{40}H_{35}Fe_4N_2O_{12}PSe_4 \cdot 0.5CHCl_3$	$C_{21}H_{17}Fe_2O_6PSe_2$
mol wt	758.14	654.00	1365.59	665.94
cryst syst	trigonal	triclinic	triclinic	monoclinic
space group	P−3	P−1	P−1	P2(1)/n
a /Å	24.751(4)	8.2595(17)	11.455(2)	12.121(2)
b /Å	24.751(4)	8.3880(17)	13.440(3)	16.884(3)
c /Å	8.7198(17)	17.727(4)	17.991(4)	12.873(3)

α /deg	90.00	103.56(3)	80.46(3)	90
β /deg	90.00	90.45(3)	74.38(3)	117.90(3)
γ /deg	120.00	102.23(3)	77.01(3)	90
V/Å^3	4626.1(13)	1164.7(4)	2583.0(9)	2326.2（8）
Z	6	2	2	4
Dc/g·cm^{-3}	1.633	1.865	1.756	1.901
abs coeff/mm^{-1}	3.343	4.409	4.084	4.481
F(000)	2268	644	1338	1304
index ranges	$-29 \le h \le 25$	$-9 \le h \le 9$	$-13 \le h \le 13$	$-14 \le h \le 14$
	$-29 \le k \le 29$	$-9 \le k \le 6$,	$-15 \le k \le 15$	$-19 \le k \le 20$
	$-10 \le l \le 8$	$-20 \le l \le 21$	$-21 \le l \le 21$	$-15 \le l \le 9$
no. of reflns	28412	7645	26567	15466
no. of indep reflns	5294	3954	9109	4096
$2\theta_{max}$ /deg	50.02	50.04	50.04	50.04
R	0.0723	0.0940	0.0757	0.0292
R_w	0.1859	0.1557	0.2087	0.0676
goodness of fit	1.034	0.675	1.048	1.069
largest diff peak and hole/e Å^{-3}	0.984/−1.226	0.973/−1.096	2.018/−1.124	0.904/−0.522

Table S5. Crystal Data and Structure Refinements Details for 8–10

	8	**9**	**10**
mol formula	$C_{25}H_{19}Fe_2O_5PSSe_2$	$C_{19}H_{15}Fe_2O_5PSSe_2$	$C_8H_4Fe_2O_7SSe_2$ ·1/2CH_2Cl_2
mol wt	732.05	655.96	556.26
cryst syst	monoclinic	triclinic	monoclinic
space group	P121/n1	P−1	C12/c1
a /Å	11.3960(10)	7.7126(15)	31.221(3)
b /Å	14.9840(12)	11.104(2)	6.9310(10)
c /Å	16.2240(15)	13.625(3)	29.758(3)
α /deg	90	102.41(3)	90
β /deg	108.920(4)	99.05(3)	97.437(4)
γ /deg	90	92.51(3)	90
V/Å^3	2620.7(4)	1121.7(4)	6385.2(13)
Z	4	2	16
D_c/g·cm^{-3}	1.855	1.942	2.315
abs coeff/mm^{-1}	4.061	4.731	6.700
F(000)	1440	640	4240
index ranges	$-15 \le h \le 14$	$-10 \le h \le 10$	$-40 \le h \le 40$
	$-19 \le k \le 19$	$-14 \le k \le 13$	$-8 \le k \le 9$
	$-21 \le l \le 18$	$-17 \le l \le 15$	$-39 \le l \le 28$

no. of reflns	23936	11148	21073
no. of indep reflns	6218	5251	7572
$2\theta_{max}$ /deg	55.86	55.74	55.74
R	0.0270	0.0627	0.0574
R_w	0.0614	0.1642	0.0857
goodness of fit	0.914	1.072	1.210
largest diff peak, hole/e Å^{-3}	0.871/−0.528	1.346/−1.304	1.051/ −0.938

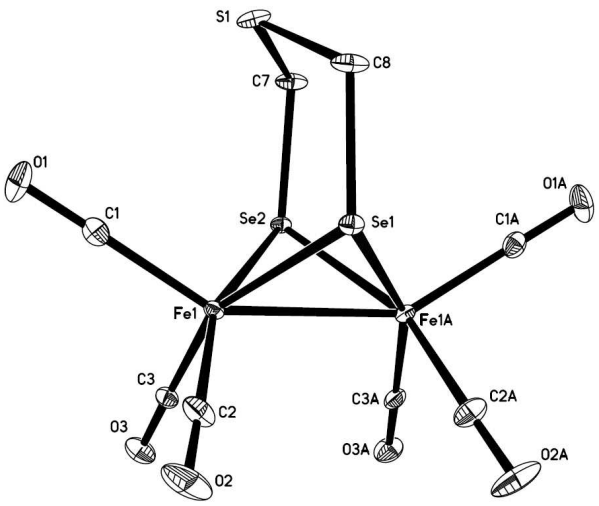

Figure S1. ORTEP view of **B** with 30% probability level ellipsoids.

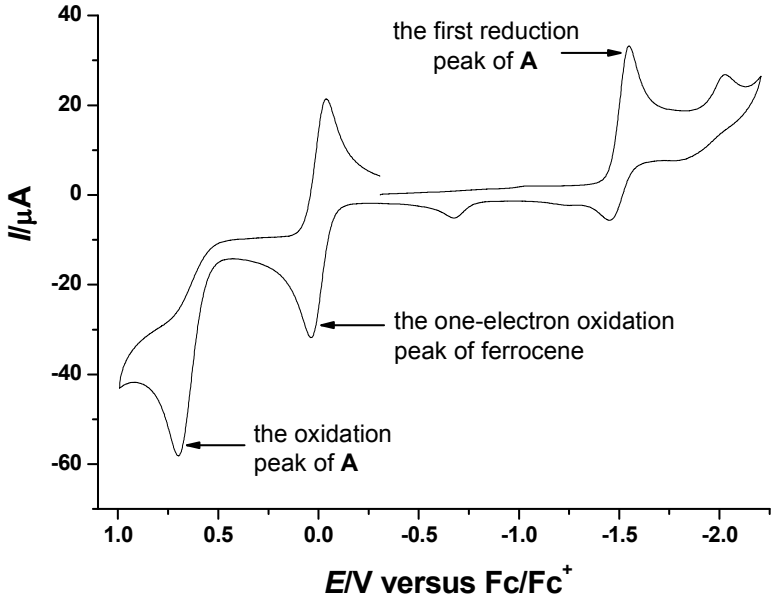

Figure S2. Cyclic voltammogram of a mixture of **A** (1.0 mM) and ferrocene (1.0 mM) in 0.1 M *n*-Bu_4NPF_6/MeCN at a scan rate of 0.1 $V \cdot s^{-1}$.

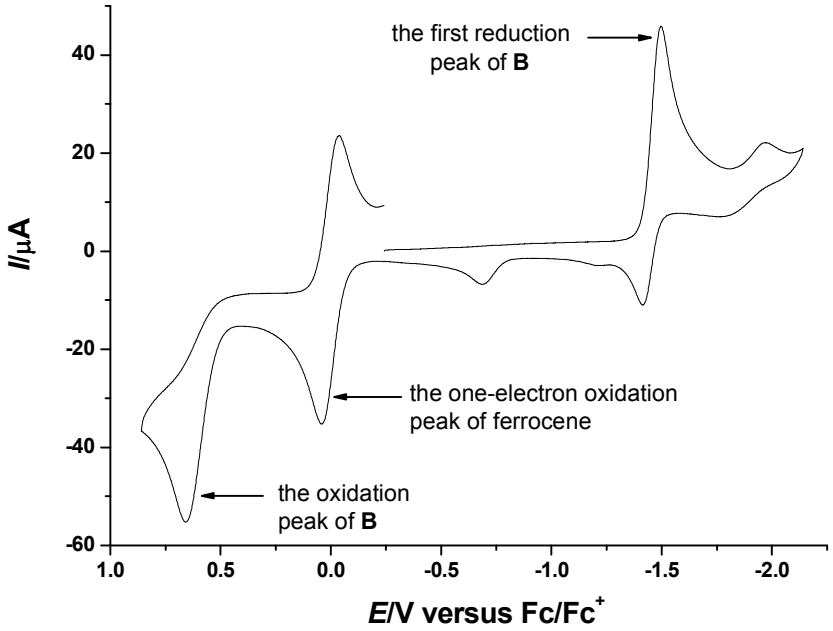

Figure S3. Cyclic voltammogram of a mixture of **B** (1.0 mM) and ferrocene (1.0 mM) in 0.1 M *n*-Bu_4NPF_6/MeCN at a scan rate of 0.1 $V \cdot s^{-1}$.

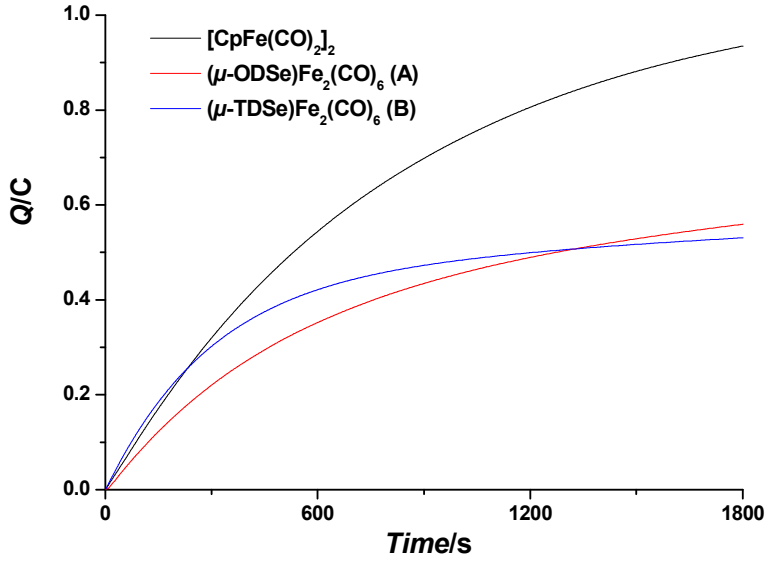

Figure S4. CPC for the two-electron reduction of $[CpFe(CO)_2]_2$ and the first reductions of **A** and **B**.

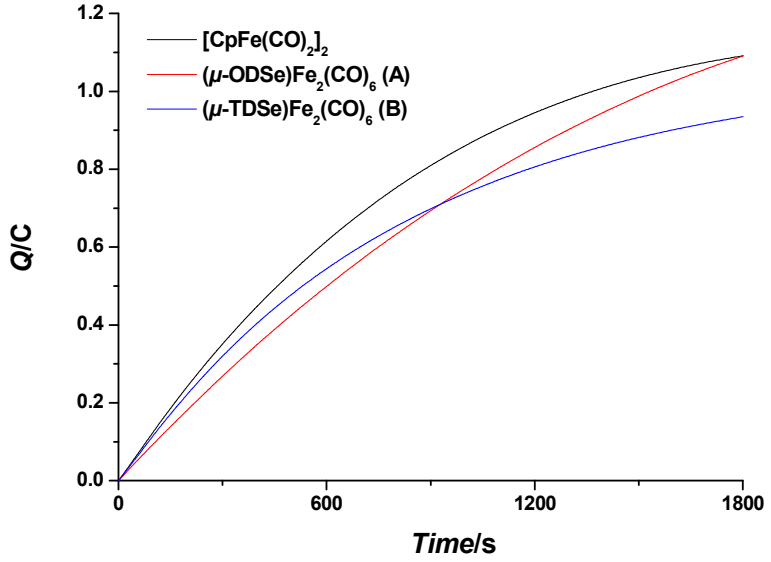

Figure S5. CPC for the two-electron reduction of $[CpFe(CO)_2]_2$ and the oxidations of **A** and **B**.

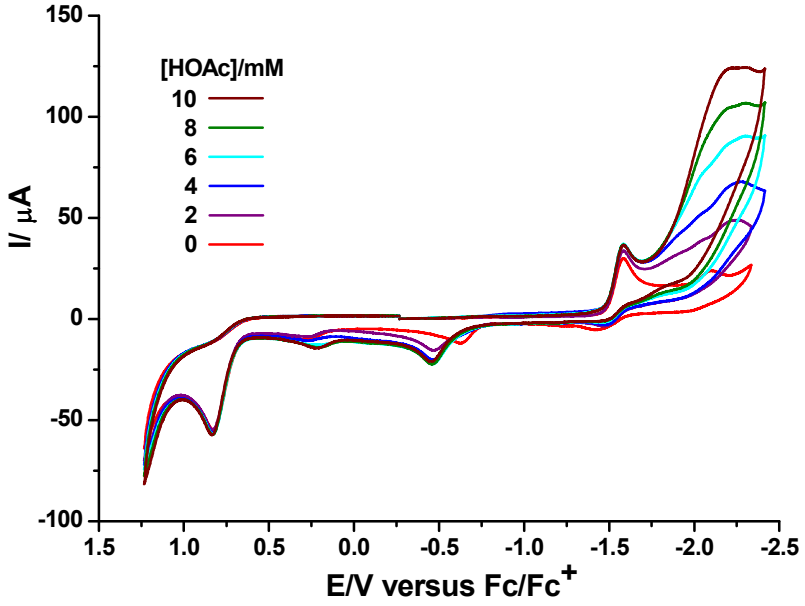

Figure S6. Cyclic voltammograms of (μ-ODT)$Fe_2(CO)_6$ (1.0 mM) with HOAc (0–10 mM) in 0.1 M n-Bu_4NPF_6/MeCN at a scan rate of 0.1 V·s^{-1}

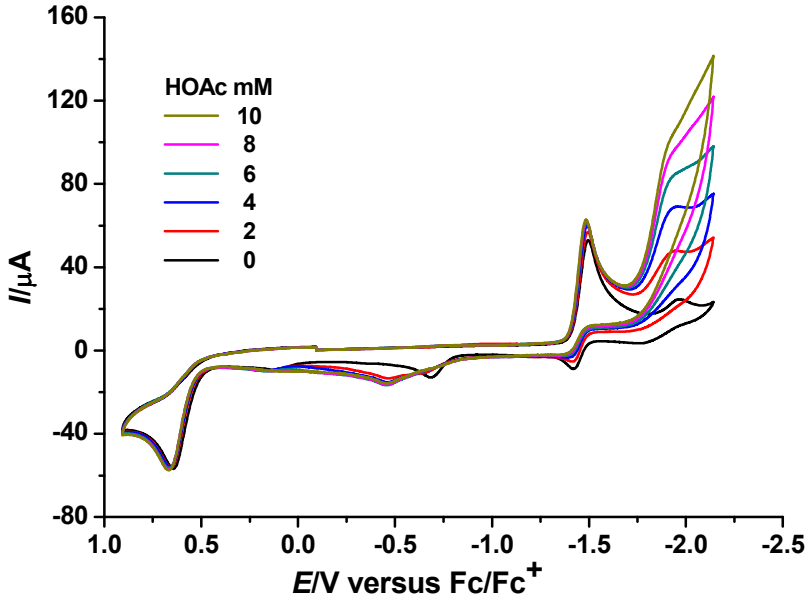

Figure S7. Cyclic voltammograms of (μ-TDT)$Fe_2(CO)_6$ (1.0 mM) with HOAc (0–10 mM) in 0.1 M n-Bu_4NPF_6/MeCN at a scan rate of 0.1 V·s^{-1}